International Journal of Advanced Research in Engineering and Technology (IJARET)
Volume 11, Issue 6, June 2020, pp. 316-327, Article ID: IJARET_11_06_028
Available online athttp://www.iaeme.com/IJARET/issues.asp?JType=IJARET&VType=11&IType=6
ISSN Print: 0976-6480 and ISSN Online: 0976-6499
DOI: 10.34218/IJARET.11.6.2020.028

STUDY OF THE FLUID DYNAMICS OF STEAM IN CEMENT AUTOCLAVE ON DIFFERENT GREEN SHEET ARRANGEMENTS AND THERMAL ANALYSIS OF GREEN SHEET

Varit Kunopagarnwong
Department of Chemical Engineering, Kasetsart University, Bangkok, Thailand

Wilawan Punkaew
Chemical Engineering Practice School, Department of Chemical Engineering, King Mongkut's University of Technology Thonburi, Bangkok, Thailand

Thongchai Rohitatisha Srinophakun*
Department of Chemical Engineering, Kasetsart University, Bangkok, Thailand
*Corresponding Author E-mail: fengtcs@hotmail.com

ABSTRACT

Portland cement, silica, gypsum, water, and the wood pulp mixed as industrial-scale fibre cement has the problem of green sheet stack damage from thermal cracking in an autoclave. This article proposes a green sheet arrangement in an autoclave to limit product damage due to non-uniform heat distribution. The fibre cement curing process was simulated by a CFD method which was divided into three parts. The first part was to understand the fluid dynamics of steam inside the autoclave and arrangement. The second part studied heat transfer inside the green sheet in two different palettes; spacer palette, and solid palette. In the third part, thermal stress from rapid cooling was studied. The results showed that an interval space of 5 cm and overlapped stacks would be sufficient because the steam temperature and pressure are maintained uniformly. The different surface temperatures in the cooling down step of no-interval stacks (scenario I) and 5 cm of interval stack (scenario II) were 24.57 and 6.22 K; respectively. The thermal cracking found in scenario I was due to the rapid cooling of the green sheet surface. The maximum deformation at the surface was about 2.3 mm. Thus, the upper layer could be damaged due to the expansion of a green sheet stack. In scenario II, the maximum stress did not develop over the ultimate stress because the space between green sheets can support the expansion.

Key words: Autoclave, curing process, green sheet arrangement, heat transfer, interval space

Cite this Article: Varit Kunopagarnwong, Wilawan Punkaew and Thongchai Rohitatisha Srinophakun, Study of the Fluid Dynamics of Steam in Cement Autoclave on Different Green Sheet Arrangements and Thermal Analysis of Green Sheet, *International Journal of Advanced Research in Engineering and Technology,* 11(6), 2020, pp. 316-327.
http://www.iaeme.com/IJARET/issues.asp?JType=IJARET&VType=11&IType=6

1. INTRODUCTION

Nowadays, the building material industry has much more competition because there are many suppliers. New technology has been applied to develop the production process of construction materials to enhance product quality. Mahaphant Fibre-Cement Public Company Limited is the leader in construction materials research and development in Thailand [1]. This is one of the largest manufacturers of fibre cement products and concrete roof tiles [2]. It has been successful; therefore, it needed to expand the capacity of its plant to increase production. The products are under the brands Ha Huang and SHERA. There are four main types of products; fibre cement tile, concrete tile, siding board, and decor stone. Fibre cement consists of Portland cement, silica sand, gypsum, water, and wood pulp [3]. All of the materials are mixed and formed a slurry. Then the slurry is formed into fibre cement by a sieve roller. After fibre cement is formed, it passes through a tunnel under ambient temperature and pressure for pre-curing. After the pre-curing process, the fibre cement tiles are sent to an autoclave where high temperature and pressure are applied for a chemical reaction between Portland cement, gypsum, and silica sand to form fibre cement products [4-5]. The final processes of fibre cement production are cutting, painting, and the packaging process. All process conditions depend on production design and customer needs. There are 22 units of the autoclave [6]. The steam consumption and time for curing in each autoclave depends on the type of product that is produced inside the autoclave. The approximate time used for curing a product is about 18 hours. The operation of the autoclave is based on the curing curve of each product. The steam feeds in slowly until 10 barg and 180 ^{o}C are reached [7]. This heating stage should be completed and the prescribed pressure reached in about 2 hours. The temperature is allowed to increase up to 180 ^{o}C in the second hour. The period of treatment under full pressure depends on the strength requirements. This period is 12 hours for fibre cement products. The steam is cut off, and the pressure is released after the completion of this stage and products are left in the autoclaves for 2 hours to cool off slowly [8-9]. The company wanted to reduce the amount of damaged product due to non-uniform heat distribution in the green sheet [10-11]. Thus, heat distribution is focusing on the fluid dynamics of steam in a cement autoclave. After that, the heat distribution in the green sheet will be analysed, and the effect of damaged product due to temperature change in a green sheet product will be studied.

The purpose of this study was to propose an appropriate green sheet arrangement to have uniform heat distribution inside the cement autoclave. Then, heat transfer in the green sheet was studied. Lastly, thermal cracking was analyzed. There are four assumptions for this study. First, the fluid dynamics of steam by different green sheet arrangements are simulated. Second, simulate heat transfer in green sheet via transient thermal option. Third, simulate the thermal stress in green sheet via the static structural option, and finally, simulate with the operating conditions of a fibre cement autoclave with more than 500,000 tons of production per year at the Fibre-Cement Public Company.

2. METHODOLOGY

2.1. Governing Equations

Three-dimensional, steady, incompressible, turbulent fluid flow with heat transfer is assumed in the system enclosure. The fluid under consideration is steam, for which constant properties are assumed in the entire computational domain. Based on the above-mentioned assumptions, the governing equations for continuity, momentum, and energy can be written in vector form as follows:

Continuity equation

$$\frac{\partial}{\partial x_i}(\rho u_i) = 0 \tag{1}$$

Momentum equation

$$\frac{\partial}{\partial x_j}\left(\rho u_i u_j\right) = -\frac{\partial p}{\partial x_i} + \frac{\partial \tau_{ij}}{\partial x_j} + \rho g_i \tag{2}$$

Where the shear stress components are given by

$$\tau_{ij} = \left[\mu\left(\frac{\partial u_i}{\partial x_j} + \frac{\partial u_j}{\partial x_i}\right)\right] - \frac{2}{3}\mu\frac{\partial u_i}{\partial x_i}\delta_{ij} \tag{3}$$

Energy equation

$$\frac{\partial}{\partial x_i}(\rho u_i h) = \frac{\partial}{\partial x_i}\left(k_{eff}\frac{\partial T}{\partial x_i} + \sum_j h_j J_j\right) + S_h \tag{4}$$

2.2. Modelling of Turbulence

For modelling turbulence, the well-known k-ε turbulence model is used [12]. The standard k-ε model is a semi-empirical model based on model transport equations for the turbulent kinetic energy (k) and its dissipation rate (ε). Non-equilibrium wall functions are used for near-wall treatment. The two differential equations that govern the transport of turbulence kinetic energy (k) and its dissipation rate (ε) are given by:

$$\frac{\partial}{\partial t}(\rho k) + \frac{\partial}{\partial x_i}(\rho k u_i) = \frac{\partial}{\partial x_i}\left[\left(\mu + \frac{\mu_t}{\sigma_k}\right)\frac{\partial k}{\partial x_j}\right] + G_k + G_b + \rho\varepsilon \tag{5}$$

$$\frac{\partial}{\partial t}(\rho\varepsilon) + \frac{\partial}{\partial x_i}(\rho\varepsilon u_i) = \frac{\partial}{\partial x_j}\left[\left(\mu + \frac{\mu_t}{\sigma_\varepsilon}\right)\frac{\partial \varepsilon}{\partial x_j}\right] + C_{1\varepsilon}\frac{\varepsilon}{k}\left(G_k + C_{3\varepsilon}G_b\right) - C_{2\varepsilon}\rho\frac{\varepsilon^2}{k} \tag{6}$$

G_k represents the generation of turbulent kinetic energy due to the mean velocity gradients, and is calculated as

$$G_k = -\rho u_i u_j \frac{\partial u_j}{\partial x_i} \tag{7}$$

G_b is the generation of turbulent kinetic energy due to buoyancy, calculated as

$$G_b = -\beta g_i \frac{\mu_t}{Pr_t}\frac{\partial T}{\partial x_i} \tag{8}$$

The turbulent viscosity, μ_t, is computed by combining k and ε as follows,

$$\mu_t = \rho C_\mu \frac{k^2}{\varepsilon} \tag{9}$$

The model constant $C_{1\varepsilon}$ and $C_{2\varepsilon}$ in Eq. (6) have the following values: $C_{1\varepsilon} = 1.44$ and $C_{2\varepsilon} = 1.92$. The value of $C_{3\varepsilon}$ is determined using the expression $C_{3\varepsilon} = \tanh|v/u|$. The turbulent Prandtl numbers for k and ε are given by $\sigma_k = 1.0$ and $\sigma_\varepsilon = 1.3$, respectively.

2.3. Creating Geometry via SolidWorks

SolidWorks is an application that is distributed along with FLUENT. SolidWorks is a tool to generate or import geometry so that it can be used as a basis for simulations run in FLUENT [13-14]. The geometry created from SolidWorks is shown in Fig. 1(a) and 1(b), while the dimensions of the autoclave model of the existing interval spaces are shown in Fig. 2(a), (b), and (c).

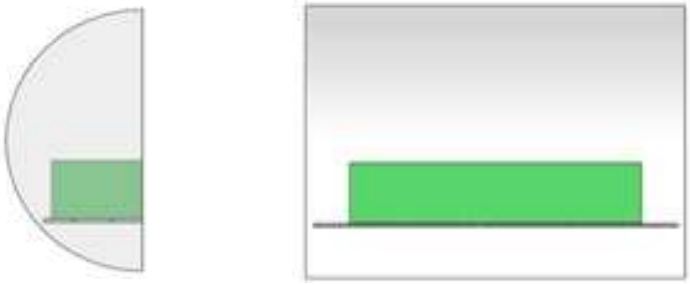

(a) (b)

Figure 1 The geometry in SolidWorks (a) Front plane (b) Right plane

Mesh of each part in the simulation would be created separately, following the physical model.

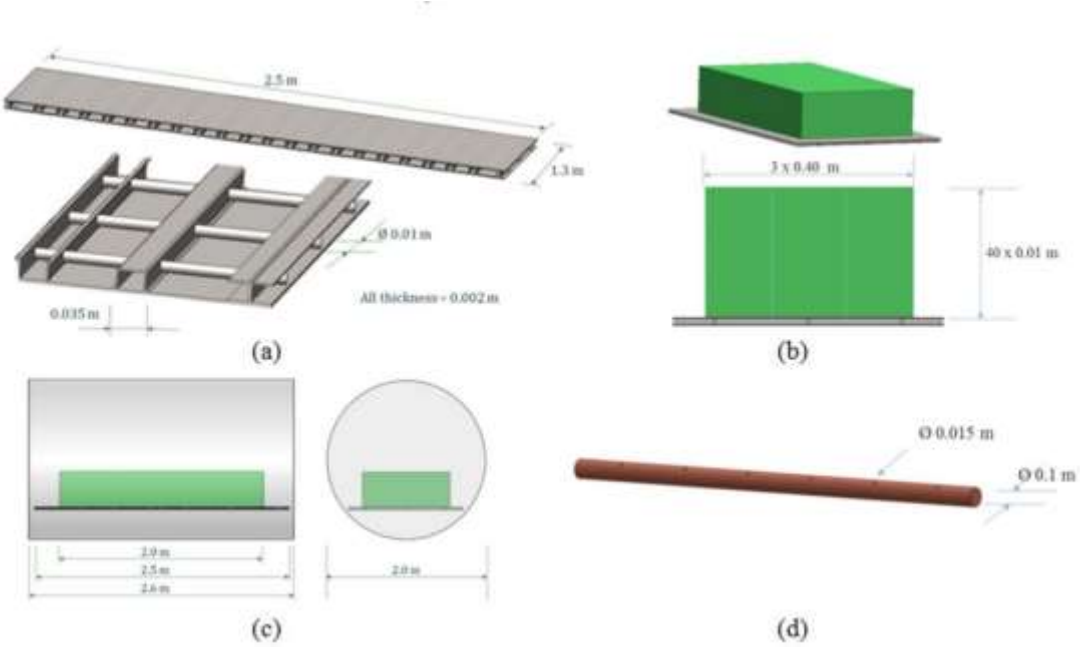

Figure 2 The geometry of a component in an autoclave (a) spacer pallet (b) green sheet (c) autoclave and green sheet (d) steam pipe

There are five cases of simulations in this study, which are no interval space, interval space 2 cm, interval space 2 cm with the overlapped stack, interval space 5 cm, and interval space 5 cm with the overlapped stack. The geometry created is shown in Fig. 3.

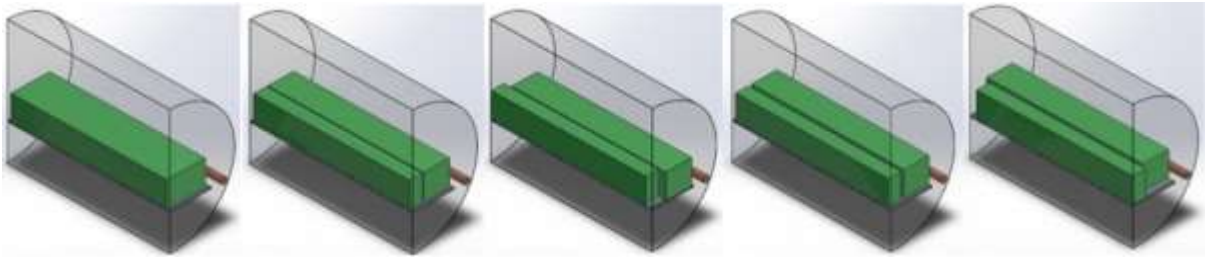

(a) (b) (c) (d) (e)

Figure 3 The geometry from SolidWorks (a) no interval space (b) interval space 2 cm (c) interval space 2 cm with overlapped stack (d) interval space 5 cm (e) interval space 5 cm with the overlapped stack.

2.4. Meshing via Ansys ICEM

The geometry needs to generate a mesh for the surface and volume of the geometry, allowing it to be used for computational fluid dynamics. Tetrahedron mesh is used to create the geometry of an autoclave because it can support the complex geometry. The mesh proposed can be diagnosed and then fixed, for example, by checking the hole, gap, and bad quality elements. The finer element can be created by adjusting the scale factor and the maximum element size. The generated mesh from ICEM is shown in Fig. 4.

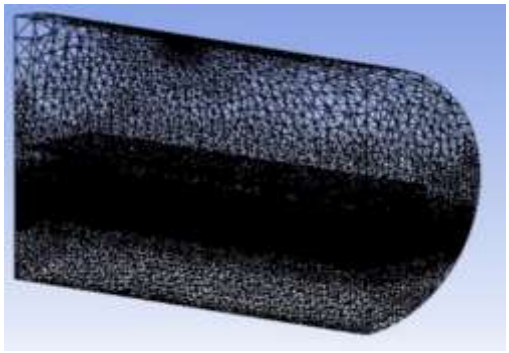

Figure 4 The generated meshes from ANSYS ICEM

2.5. Boundary Conditions

The boundaries of the fluid domain that need to be specified are inlet, outlet, and wall. In this thesis, the inlet velocity magnitude of 10 m/s is defined, the temperature of inlet steam is 453 K, and the pressure is 1.01 MPa. Then the outlet vent is 303 K. The autoclave model is assumed to be adiabatic to control the operating temperature inside the autoclave. To verify this assumption, a CFD simulation including the energy equation has been run.

According to the autoclave simulation with existing interval spaces, the geometry of an autoclave is modified by varying the green sheet arrangement inside the fibre cement autoclave in order to increase steam distribution. This simulation is under the following assumptions:

- The green sheet is homogeneous.
- The steam flow is turbulent flow.
- The geometry of autoclave is symmetry.

The thermal cracking was simulated via transient structural to analyze the stress due to temperature change. The temperature from the operating curve was applied to the green sheet. There were two scenarios to simulate in this step.

3. RESULT AND DISCUSSION

3.1. The Velocity Profile of Steam

In this study, the fluid dynamics was the first step in the simulation to get a better understanding of the SolidWorks and Fluent program. Steam was used as the working fluid and operation was at 10 bars and 180°C. The operating curve during the first two hours shows the temperature and pressure rising step. The inlet velocity from 6 holes was set as 10 m/s, and there was a vent hole at the top of the autoclave. The velocity after two hours of the temperature and pressure rising steps is illustrated in Fig. 5.

The velocity distribution in the autoclave is discussed in this section. In all scenarios, the steam flowed through every location. The steam comes from an inlet hole at high velocity (about 10 m/s) and then hits the green sheet stack and autoclave wall. As a consequence, the momentum in a fluid is transferred to the wall and green sheet. Owing to this reason, the velocity suddenly decreased after hitting the wall and green sheet. However, the difference in each scenario was the location of the green sheet stack. In all scenarios, the velocity was the movement at the top of the green sheet in the autoclave because the steam inlet hole was flowing upward. On the other hand, the velocity was not transferred to the bottom of the autoclave because the palette obstructed the steam transfer. After two hours of the temperature and pressure rising step, it was shown that the velocity was entirely inside the autoclave, including within the space of the palette.

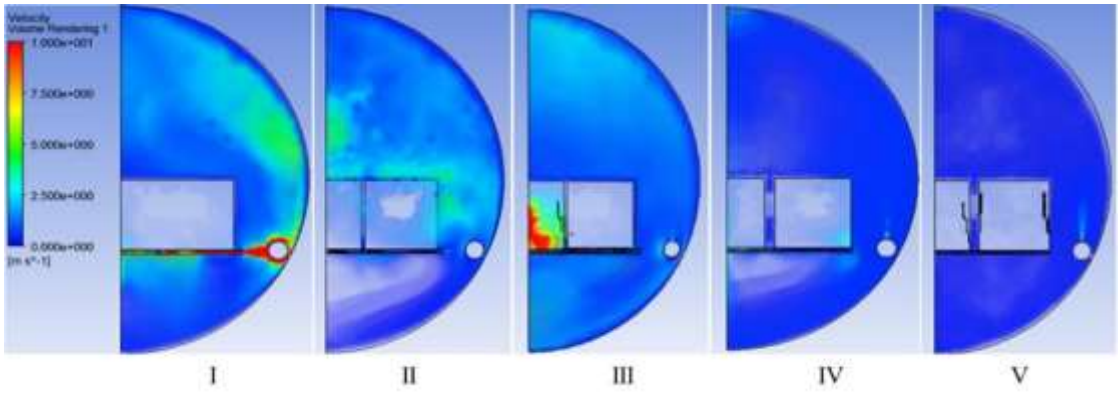

Figure 5 Velocity profile of steam in an autoclave (I) No interval space (II) Interval spaces 2 cm (III) Interval spaces 2 cm with overlapped stack (IV) Interval spaces 5 cm (V) Interval spaces 5 cm with an overlapped stack

Theoretically, after two hours of the temperature and pressure rising step, the temperature and pressure should be 453 K and 1.01 MPa, respectively. The average temperature in the autoclave with the scenario I to V is shown in Table 1. In all situations, the temperature and pressure rose to about 453 K and 1.01 MPa, respectively. The results were in agreement with the operating conditions of the operating curve.

Table 1 Temperature and pressure of steam in an autoclave

Scenario	Temperature (K)	Pressure (MPa)
II) Interval spaces 2 cm	451.39	1.015
III) Interval spaces 2 cm with an overlapped stack	451.54	1.017
IV) Interval spaces 5 cm	450.14	1.018
V) Interval spaces 5 cm with an overlapped stack	452.54	1.015

3.2. The Temperature Distribution in the Green Sheet

The fluid dynamics of steam flow in the autoclave were already studied in the Fluent program. The temperature distribution inside the green sheet was studied later in Transient thermal, which is one option in ANSYS. In this part, there was a study of the temperature distribution in green sheet when using different palette types, which are solid palette and spacer palette.

Before studying heat distribution in green sheet, heat transfer in the palette was simulated by increasing the temperature from 303 to 453 K in two hours.

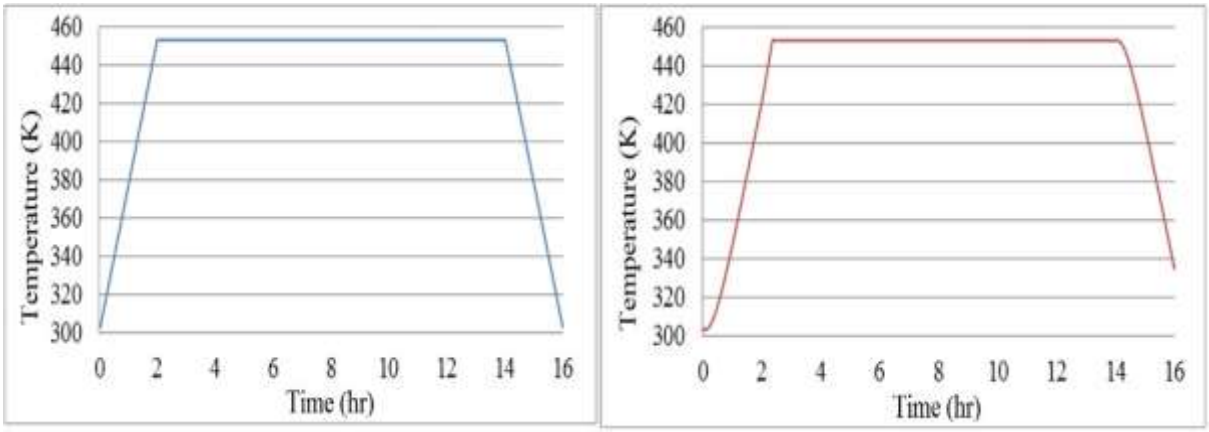

Figure 6 The temperature profile of spacer pallet and solid pallet

These temperature profiles were used to heat the green sheet at the bottom of the green sheet stack, as shown in Fig. 6 for spacer palette and solid palette, respectively. The other 5 surfaces of green sheets used the temperature of scenario V from the previous part. After that, the temperature profile was applied to the surface of the green sheet. In this part of the study, there are 2 scenarios of green sheet arrangement—combined three stacks and only one stack of the green sheet. The temperature distribution of scenarios I and II is shown in Fig. 7.

The temperature of the two scenarios due to the difference of palette types shows the following: after the end of the temperature raising step (2 hr), the bottom of the green sheet on the solid palette does not reach 453 K. Time for curing at 453 K was less than each scenario. It resulted in non-uniform heating of the green sheet. Moreover, after the cooling down step is finished, the temperature at the bottom of the green sheet on a solid palette was still high. When this product is transferred out of the autoclave, it can be damaged. Thus the spacer palette should be used to cure the green sheet.

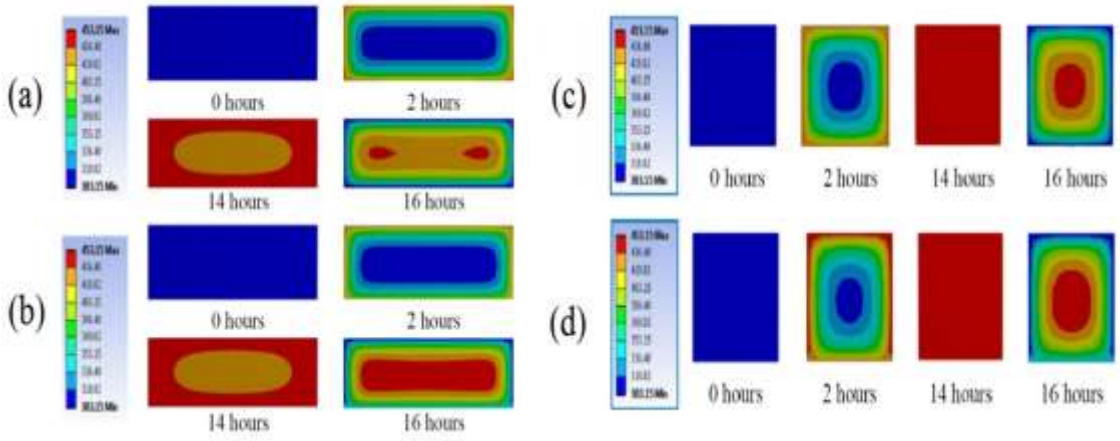

Figure 7 The temperature distribution inside green sheet (a) scenario I on spacer pallet (b) scenario I on solid pallet (c) scenario II on spacer pallet (d) scenario II on solid pallet

This section will consider green sheet curing on a spacer palette for 2 scenarios. The maximum temperature was the temperature, which is heated at the surface of the green sheet stack. In the cooling-down step, the maximum temperature means the highest temperature inside a green sheet or at the center of a green sheet. The scenario I referred to as the combined three stacks of the green sheet. The temperature was increased until it reached 453 K, while the final temperature at the centre of the green sheet after it cooled down from the maximum temperature to 428 K.

The temperature distribution of scenario II is referred to as one stack of the green sheet. The temperature was increased until it reached 453 K while the final temperature at the centre of the green sheet after it cooled down from 453 K was 447.05 K. This scenario shows that temperature at the centre of the green sheet stack increases faster than the combined three stacks in scenario I.

When the surface temperature deviates greatly from that of the core, thermal cracking will develop. The surface temperature of the green sheet in the scenario I decreased from 453 to 428.43 K. The difference in temperature was 24.57 K. In scenario II, the difference in surface temperature after the cooling down step was 6.22 K. The difference in temperature between the surface and the central of scenario II was higher than one so that the green sheet could be damaged due to the rapidly cooling down of the green sheet surface as shown in Fig. 8.

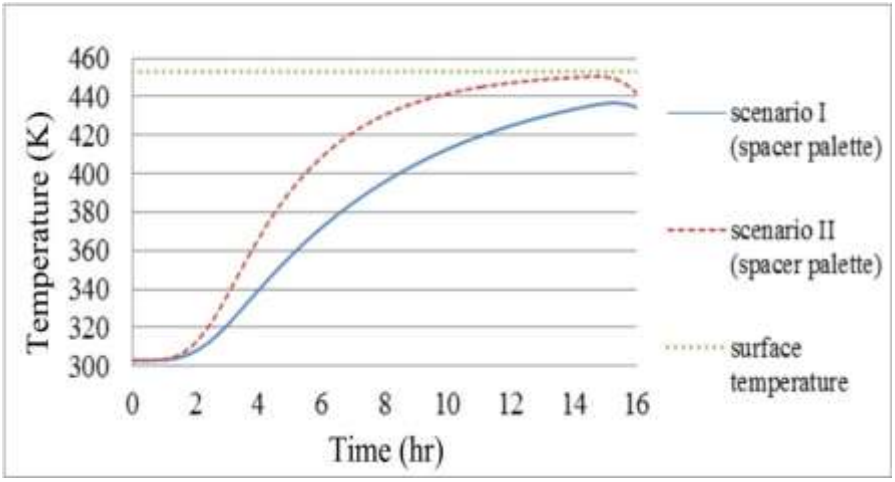

Figure 8 A comparison between the central temperature inside a green sheet in scenarios I and II

3.3. The Possibility of Thermal Cracking in the Green Sheet

When heat is applied to any material, the result is thermal stress in that material. In green sheet sections, the internal temperature rises and drops slowly, while the surface cools rapidly to ambient temperature. The hotter interior green sheet restrains surface contraction due to cooling, and it did not contract as quickly as the surface. This restraint created stress that can crack the surface of the green sheet. Thermal cracking can occur when the concrete surface was exposed to extreme temperature quickly.

The Scenario I: Combined three stacks of the green sheet

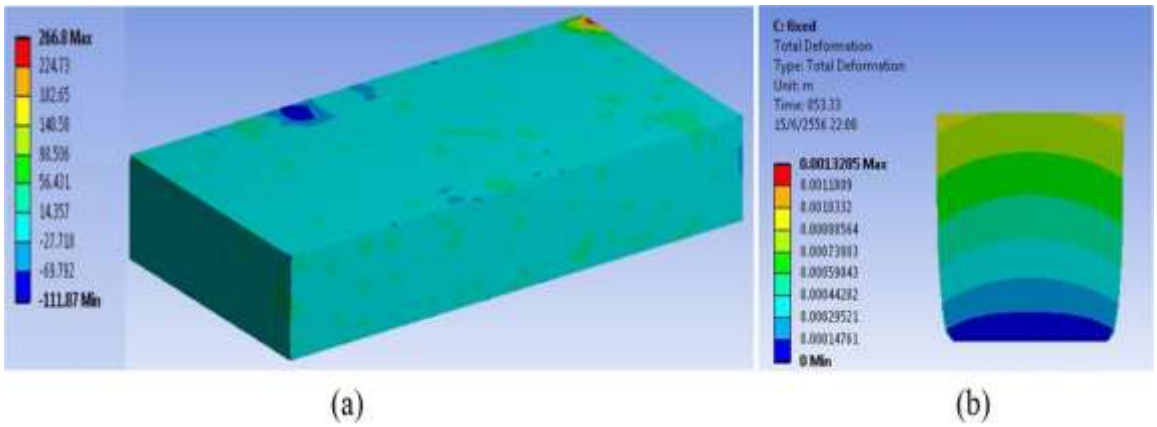

Figure 9 CFD result of the green sheet in the scenario I (a) the position of maximum stress (b) the deformation of the green sheet

The stress of hard fibre cement board cannot accept more than the ultimate stress, 51.2 MPa. When the stress is more than the ultimate stress, the result is the fracture of the product. The combined three-stack results showed that the maximum stress was higher than the ultimate stress for 4 layers. The heat was applied to 6 surfaces while the bottom surface was fixed because it was in contact with the palette. The deformation of the green sheet would expand normal to the surface and maximum at the surface. The maximum deformation at the surface was about 1.3 mm (Fig. 9(b)). Thus the upper layer could be damaged due to the expansion of a green sheet stack. The total number of green sheets that could be damaged from higher stress due to rapid cooling was twelve sheets.

Scenario II: One stack of the green sheet

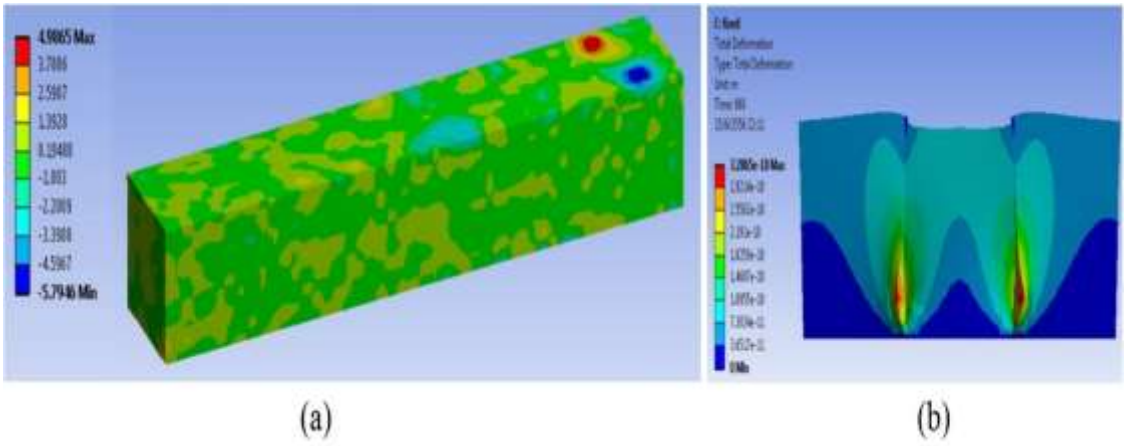

Figure 10 CFD result of the green sheet in scenario II (a) the position of maximum stress (b) the deformation of the green sheet

In scenario II, one stack of the green sheet, after the heat was applied to the entire surface of the stack, the maximum stress did not exceed the ultimate stress. The maximum stress and the position of green sheets that are stressed more than the ultimate stress of scenario II were shown in Fig. 10. Thus, the combined three stacks of the green sheet should be separated into individual stacks to decrease the maximum stress so that it is not over the ultimate stress.

4. CONCLUSION

In this work, a CFD model of green sheet curing in an autoclave was simulated to find the optimum green sheet arrangement for decreasing damaged product from the curing process. The results of the CFD simulation was divided into three parts: the effect of fluid dynamics on green sheet arrangement, heat transfer in green sheet, and thermal stress analysis. The first part was developed to understand the fluid dynamics of steam inside the autoclave. The steam was inlet from holes of a steam pipe at 453 K and 1.01 MPa. The green sheet arrangement was such that the interval space was 5 centimetres and the overlapped stack was selected. After two hours of the temperature and pressure rising step in the operating curve, the results of this arrangement were uniform temperature and pressure in the cement and the autoclave at 452.5 K and 1.015 MPa, respectively, that was close to the operating curve of the curing process. In the second part, heat transfer inside the green sheet was studied. The temperature at the palette and steam was 453 K, and 1.01 MPa from previous the simulation, including the operating curve, was applied in this simulation. The difference in surface temperature during the cooling down step of the combined three stacks and each stack was 24.57 and 6.22 K, respectively. Thermal cracking could occur in the combined three stacks due to the rapid cooling down of the green sheet surface. The third part studied the thermal stress from rapidly cooling from the second part. The temperature was applied by using an operating curve again. The combined three-stack results have shown that the maximum stress was higher than the ultimate stress for four green sheet layers. The heat was applied to six surfaces while the bottom surface was fixed because it was in contact with the palette. The deformation of the green sheet would expand normally to the surface and maximum at the surface. The maximum deformation at the surface was about 2.3 mm. Thus the upper layer could be damaged due to the expansion of a green sheet stack. The total number of green sheets that could be damaged from higher stress due to rapid cooling was twelve sheets.

In conclusion, an interval space of 5 centimetres and an overlapped stack would be preferred, because the steam temperature and pressure were uniforms. After the operating temperature was applied to a green sheet, the surface temperature was not changing too rapidly. When the thermal stress was analyzed, the maximum stress was not exceeding the ultimate stress, and the space between green sheets could support the expansion due to deformation from heating.

5. NOMENCLATURES AND GREEK SYMBOLS

$C_{1\varepsilon}$ k-ε model constant

$C_{2\varepsilon}$ k-ε model constant

$C_{3\varepsilon}$ k-ε model constant

g acceleration due to gravitational force, 9.81 m/s^2

G_b generation of turbulent kinetic energy due to buoyancy, kg/m s^2

G_k generation of turbulent kinetic energy due to the mean velocity gradients, kg/ms^2

h sensible enthalpy, J/kg K

J diffusion flux of species, j

k turbulent kinetic energy, m^2/s^2

k_{eff} effective thermal conductivity of the fluid, W/m K

Pr_t turbulent Prandtl number

t time, s

T temperature, ^oC

6. GREEK SYMBOLS

β coefficient of thermal expansion, 1/K

δ Kronecker delta

ε dissipation rate of turbulent kinetic energy, m^2/s^3

μ dynamic viscosity, Ns/m^2

μ_t turbulent viscosity, Ns/m^2

ν kinematic viscosity, m^2/s

σ_ε turbulent Prandtl number for ε

σ_k turbulent Prandtl number for k

τ shear stress, N/m^2

τ_w wall shear stress, N/m^2

ACKNOWLEDGMENTS

Wichit Prakaypan Mahaphant Fibre-Cement Public Company Limited, Lopburi and Faculty of Engineering Kasetsart University Thailand have supported this research.

REFERENCES

[1] W. Keadsuk, (2008) Fibre-cement introduction, Mahaphant Fibre Cement Group.

[2] Mahaphant Group, (2012) Mahaphant History. www.Mahaphant.com, 2008. (accessed May 26, 2012).

[3] M.S. Gani, (1997) Cement and concrete, Hydration of Cement-setting reactions, 3 (Chapman & Hall, London, 1997) 36-46.

[4] P. Bazant, P. Zdenek, (1996) Concrete at high temperature: material properties and mathematical models, Curing Concrete, Longman Group, Essex, 12, 219-228.

[5] M.L. Gambhir, (2004) Concrete Technology, Handbook of Civil engineering series, 3 (New Delhi, Tata McGraw-Hill, 2004) 304-307.

[6] Acmega Co. Ltd, (2008) Basic Knowledge of Autoclave and Retort.

[7] W. Jeffrey, A. Bullard, M.J. Hamlin, A.L. Richard, N. Andre, W.S. George, S.S. Jeffrey, L.S. Karen, J.T. Jeffrey, (2011) Mechanisms of cement hydration, Cement and Concrete Research, 41(12), 1208-1223.

[8] L. Min, L.T. Charles, (1999) Optimal Curing for Thermoset Matrix Composites: Thermochemical and Consolidation Considerations, Department of Mechanical and Industrial Engineering, University of Illinois, Urbana, Illinois.

[9] P.C. Taylor, (2006) Integrated Materials, and Construction Practices for Concrete Pavement: A State-of-the-Practice Manual, Ames, Iowa, Iowa State University, 69-104.

[10] Q.C.A. Chen, J. Mayers, Van der Kooi, (1989) Convective heat transfer in rooms with mixed convection, International Seminar on Indoor Air Flow Patterns, University of Liege, Belgium, 69-82.

[11] A.M. Cooke, (2005) The Measurement and Significance of Green Sheet Properties for the Properties of Hardened Fibre Cement, Cement and Concrete Composites, 27(5), 604-610.

[12] J.E. Bolander, M. Yip, (2012) Numerical modelling of fibre reinforced cement composites subjected to drying, Modeling, and simulation, the University of California at Davis, USA, 1, 7-20.

[13] ANSYS Inc., (2012) FLUENT 12.0 User's Manual, (ANSYS Inc. USA, 2012).

[14] T. Jiyuan, H.Y. G, L. Chaoqun, (2008) Computational Fluid Dynamics, (UK, 2008) 29-63.